

A Robotic Surgery Exploration Arrangement for Hepatic Microwave Coagulation Therapy

S. Boopathi Raja*, S. Arasu, B. Jaiganesh

Department of Electronics & Communication Engineering, Saveetha School of Engineering, Chennai, India

*Corresponding author email: thalaraja999@gmail.com

ABSTRACT

This paper counseled a needle insertion robotic surgery arrangement for hepatic microwave coagulation of liver tumors. The arrangement might compensate the impact provoked by the patient's respiratory motion. The arrangement includes a needle insertion robot, a surgical arranging subsystem, a magnetic pursuing mechanism and a stereo vision system. In order to encounter the frank necessity of the arrangement, inserting the needle precisely to the target, we counseled a method in this paper. First, a patient body fixation method was utilized to cut unintentional patient movement. Then, stereo vision method was utilized to trail the markers on the patient's body surface. By joining the fixation and stereo vision, we can draw the precise gesture of the structure, minimizing impact of respiratory and cardiac motion. Finally, accuracy examination on 3D ultrasound phantom was grasped out to assess the exploration system. The aftermath indicated that the counseled method might enhance arrangement accuracy, enhancing the efficiency of interference therapy for the hepatic tumors and cutting the patient's pain.

Keywords - Robotic exploration, arrangement accuracy, stereo vision.

1. INTRODUCTION

Hepatic (liver) cancer reasons the most demises for patients alongside hepatopathy. Current treatments for hepatic cancer are liver resection (surgical removal of a serving of the liver, whereas the liver tumor s are located) or ablative treatment. Unfortunately, most patients alongside main or secondary liver cancer are not candidates for the resection method, generally due to the tumor s locale or underlying liver diseases. For these reasons, there has been an rising attention in Interventional Radiology (IR) for ablation treatment of hepatic tumor s, that might cut the period expenditure of the hospital treatment and the pain of patients. Contrasted alongside standard open surgery, the IR method does not need laparoscopy. In IR treatment, Microwave Coagulation Therapy (MCT) or Ethanol Inoculation Therapy (EIT) is given below picture guidance methods, such as Computed Tomography (CT), Magnetic Resonance (MR), Ultra-Sound (US), etc. Amid these methods, US picture is the prime candidate because it can furnish brilliant real-time anatomical imaging and distinctive adaptability in the multitude of interventions. Though, due to the limitation of 3D vision monitoring of the target tumor s and the needle insertion trail, these procedures frequently need exceedingly experienced skills and familiarize supplementary burden to the surgeon, thus weakening the treatment result due to missing the target

or inaccurate positioning of the needle. Recently, countless researches on needle insertion instrument for the MCT of hepatic cancer have been reported. Doctor and Taylor industrialized a dual-armed robotic arrangement that grasped both the ultrasound manipulation and the needle guidance to vanquish the setback of freehand US method, for intra-operative ultrasound-guided hepatic ablative therapy. Hong et al counseled a gesture flexible needle allocating instrument encompassed of a five DOF (degree of freedom) passive arm, accompanied by tumor segmentation in ultrasound pictures. Besides, supplementary intellectual and scrutiny clusters have industrialized the comparable systems. For example, Abolmaesumi industrialized a robot-assisted arrangement for health diagnostic ultrasound. Chung counseled a robot-assisted surgery for spinal mixture. In neurosurgery and orthopedics surgery, the rigid structures are frequently believed nearly immobile. Though, in the earth of abdominal interference surgery, the structures move and deform due to respiratory and cardiac motion. As a consequence, the precise locale of the tumor and acquaintance tissue like boat will be affected. This will make the exploration in abdominal surgery for extra difficult. Zhai gave a respiration monitoring arrangement to the procedure. A contraption was utilized to compute the number of air inhaled and exhaled by the patient. Though, the arrangement might not give the precise displacement of the organ. In

supplement, it was luxurious and colossal in size. In this paper, we counsel a robotic surgery exploration arrangement to cut the impact of movement and deformation of the flexible organs. First, patient fixation method will be utilized to cut each patient movements comparative to the pose pursuing mechanism. Second, stereo vision method is utilized to trail the markers on the patient body to recognize the movement of body surface. Even though this method might not vanquish setback gave by the respiratory gesture completely, though, it might enhance the needle insertion accuracy effectively. The rest of this paper is coordinated as follows. In serving II, the finished arrangement design will be given as the surgical arranging subsystem and the needle-insertion robot will be described. Factors altering the needle insertion accuracy will be analysed in serving III. Experimental aftermath and conclusion will be given in serving IV and V respectively.

2. ARRANGEMENT ARCHITECTURE

The robotic surgery arrangement might minimize the impact of the movement and deformation of patient body provoked by the respiration and cardiac gesture across the procedure. Fig 1 is the design of the crafted robot-assisted interference therapy arrangement industrialized in Robotics and Automation Lab of Tsinghua University. Main constituents are delineated as follows:

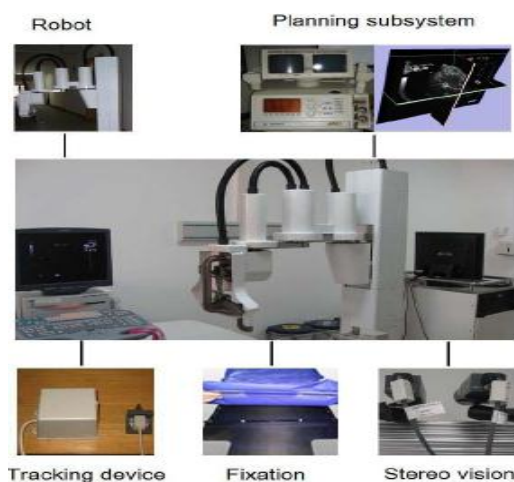


Fig. 1 Finished arrangement architecture

(1) A five DOF alert robot alongside a three DOF alert arm is utilized to escort a two DOF passive manipulator to the wanted locale on the skin. The manipulator is utilized to manipulation the access association of the needle and the distance from the needle tip to the target. Every single combined of the robot is installed

alongside a motor and an optical encoder recording the combined angle.

(2) A surgical arranging subsystem provides all the graphic interfaces, encompassing the real-time 2D and 3D US images. The arrangement is generally composed of a standard US contraction and a PC-based graphic workstation related to the analog output seaport of the contraction by a frame-grabbing card.

(3) A magnetic pursuing mechanism (MTD, PciBird, ideal 6D FOB, Ascension Knowledge Inc.) is encompassed of a transmitter fixed alongside respect to the globe coordinate in procedure and the receivers that can be freely moved. Both the locale and the orientation of the receiver can be pursued in the transmitter coordinate frame. The transmitter and the receiver delineate two different coordinate constructions that are connected by a makeover matrix. In our arrangement, the MTD transmitter is installed on the robot's center and the coordinate construction described by the MTD transmitter is believed as the globe coordinate construction all across this paper. Thus, this pursuing mechanism can be utilized to trail the probe of the US contraction, the stylus tip, the stereo vision arrangement, the procedure instruments, etc.

(4) A patient fixation (BodyFix™, Health Intelligence, Schwab-Munich, Germany) is utilized to fix the patient, cutting each patient movement comparative to the magnetic pursuing device. It uses so-called double-vacuum sandwich method and is consisted of a vacuum mattress, a cover foil and a pump. The patient is fitted to the vacuum mattress and the cover foil is next allocated on the patient. Vacuum the air in the mattress and the air amid the patient and the fixation foil by the impel, sandwiching the patient amid the foil and mattress. As a consequence, the patient is fixed securely and moderately static alongside respect to the reference globe coordinate fame and robot.

(5) A stereo vision subsystem (two SONY XCD-X710 video cameras alongside FUJINON TV LENS) is utilized to trail the markers on the patient body surface. The comparative locale amid these two video cameras is fixed. A MTD receiver can be climbed to trail the locale and orientation of this stereo vision arrangement in the transmitter's coordinate construction (the globe coordinate frame). For simplification, the stereo vision arrangement can be fixed alongside the MTD transmitter and the spatial connection amid them can be recognized by the calibration method that will be debated afterward in pursuing section. Then, we can

trail the coordinates of every single marker in the globe construction by employing a little coordinate transformations. As a consequence, the deformation and movement of the patient body external can be ambitious by the locale of these markers. We accept that the structure in the body has the alike movement as the body surface. Therefore, the procedure accuracy can be enhanced by drawing the movement of the body external from the computer monitor.

Fig 2 displays the coordinate makeover of our robotic system. The MTD transmitter construction is believed as the globe coordinate construction in the system. In this case, all the coordinates will be transformed into the T frame. The 3D US picture is industrialized across scanning the patient body by employing the probe alongside receiver fixed on it. Thus, the coordinate of every single pixel in the 3D US picture can be obtained afterward 3D US calibration. Similarly, the makeovers amid the stereo vision arrangement construction, the robot construction and the transmitter construction are additionally obtained by calibration.

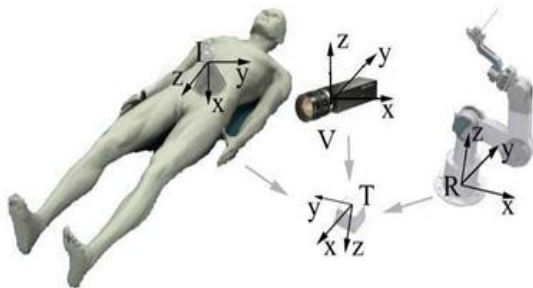


Fig. 2 The coordinate transformation

3. CLINICAL PROCEDURE

After comprehensive earth discover and discussion alongside the surgeon, we counseled a clinical procedure for our robotic surgery exploration arrangement, which will be delineated as follows.

(1) Patient fixation and instruments set-up: the patient is allocated on the surgical bed and fixed by the patient fixation system. The robotic surgery arrangement is allocated close to the projected entry point of the needle insertion. Adjust the video cameras to safeguard that all the markers on the patient body external are in the cameras' think field.

(2) Import pre-operative picture data: the procedure trail arranging and microwave warmth simulation are led beforehand operation. All these data is imported into the system.

(3) Preparation of trajectories: in order to escort the surgeon procedure, the projected procedure trail ought to be mapped to the patient physical body so that the registration is needed. The markers on the patient body external are utilized for registration. Then, the real-time US pictures are scanned to safeguard that the pre-operative ideal is accurately mapped to the patient physical body. Later that, the stereo vision arrangement will record present state and save it as the reference state.

(4) Needle inserting procedure navigation: the robot moves smoothly below the education of the computer. Next the surgeon will ask the patient to inhale or exhale air safeguarding the markers on the body external are close plenty to the reference state. The surgeon will next ask the patient to grasp his or her gulp and use real-time US scanning once more to check that it is appropriate to insert the needle at this moment.

(5) Microwave coagulation: the locale of the needle can be pursued by the MTD receiver attached to it and the real-time data will be displayed in the computer monitor afterward a little calculation. After the needle has grasped the wanted target (read from the real-time picture on the monitor), the surgeon will coil on the microwave purpose of the inserted needle to destruct the target tumors.

4. STEREO VISION

4.1 Principle of Body External Tracking

In order to enhance the needle insertion accuracy, we demand to notice the movement of the target tumor in the abdominal interference surgery. Recall the aforementioned assumption that the structure in the body has the alike movement as the body external, so, we can guesstimate the gesture of abdominal structure by pursuing the gesture of the markers on the patient body surface. We use stereo vision method as shown in Fig.3 to trail the markers.

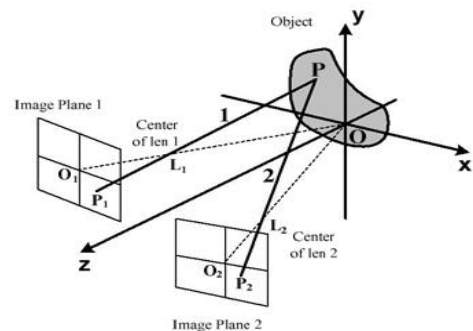


Fig. 3 Stereo vision

The comparative locale of these video cameras is fixed. An arbitrary point P in the object is projected onto point P1 and P2 in the picture plane of every single camera, as delineated by line L1 and L2, respectively. In our case, the point P is the marker in the patient's body surface. The setback is that how we can become the 3D coordinate of every single marker from these two video cameras. Following is the approach. We use the camera ideal in, that can be expressed as follows

$$s \begin{bmatrix} r \\ c \\ 1 \end{bmatrix} = \begin{bmatrix} m_{11} & m_{12} & m_{13} & m_{14} \\ m_{21} & m_{22} & m_{23} & m_{24} \\ m_{31} & m_{32} & m_{33} & 1 \end{bmatrix} \begin{bmatrix} x \\ y \\ z \\ 1 \end{bmatrix} = C \begin{bmatrix} x \\ y \\ z \\ 1 \end{bmatrix} \quad (1)$$

where s is the scale factor; [r c 1]^T is the homogeneous coordinate of the pixel in the picture frame; [x y z 1]^T is the homogeneous coordinate of the corresponding marker in the globe frame; the camera matrix C equals to the spot product of the camera extrinsic parameter matrix and intrinsic parameter matrix that can be obtained by camera calibration. By removing the homogeneous scale s in equation (1), we can attain the pursuing linear equations:

$$\begin{cases} r = (m_{11} - m_{31}r)x + (m_{12} - m_{32}r)y + (m_{13} - m_{33}r)z + m_{14} \\ c = (m_{21} - m_{31}c)x + (m_{22} - m_{32}c)y + (m_{23} - m_{33}c)z + m_{24} \end{cases} \quad (2)$$

Similarly, the marker in the subsequent camera can be expressed as the pursuing linear equations:

$$\begin{cases} p = (n_{11} - n_{31}p)x + (n_{12} - n_{32}p)y + (n_{13} - n_{33}p)z + n_{14} \\ q = (n_{21} - n_{31}q)x + (n_{22} - n_{32}q)y + (n_{23} - n_{33}q)z + n_{24} \end{cases} \quad (3)$$

Once given the camera matrices of these two video cameras, the coordinate of point [x y z]^T can be obtained by resolving each three of these equations in (2) and (3). Though, due to errors in camera ideal and the pixels in the picture plane, line L1 and L2 computed by preceding equations will usually not intersect in the 3D space. A larger way is to compute the distance amid these two skew lines, i.e., the shortest line segment relating them, as shown in Fig 4.

If the distance amid these two lines is less than the pre-defined threshold, the midpoint of the line segment will be believed as the intersection point of these two lines. If the distance exceeds the threshold, meaning the relation amid the markers and the corresponding pixels in the picture plane has a little setback and demand to

be notified, re-calibration of the video cameras or more investigation will be needed.

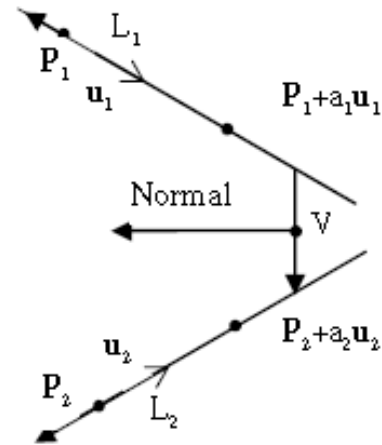


Fig. 4 The shorted distance between two skew lines

In Fig 4, P1 and P2 are the points in the picture plane; u1 and u2 are corresponding constituent vectors alongside the line L1 and L2, respectively; V is the shortest vector relating line L1 and L2 and its length equals to the distance amid these two lines. Obviously, V is perpendicular to both u1 and u2, consequently, we can derive the pursuing equations:

$$\begin{cases} ((P_1 + a_1u_1) - (P_2 + a_2u_2)) \cdot u_1 = 0 \\ ((P_1 + a_1u_1) - (P_2 + a_2u_2)) \cdot u_2 = 0 \end{cases} \quad (4)$$

From the equation (4), a1 and a2 can be solved:

$$\begin{cases} a_1 = \frac{(P_2 - P_1) \cdot u_1 - ((P_2 - P_1) \cdot u_2)(u_1 \cdot u_2)}{1 - (u_1 \cdot u_2)} \\ a_2 = \frac{((P_2 - P_1) \cdot u_1)(u_1 \cdot u_2) - (P_2 - P_1) \cdot u_2}{1 - (u_1 \cdot u_2)} \end{cases} \quad (5)$$

Then, the shortest line vector is:

$$V = (P_1 + a_1u_1) - (P_2 + a_2u_2) \quad (6)$$

So, the coordinate of the marker is

$$[x \ y \ z]^T = ((P_1 + a_1u_1) + (P_2 + a_2u_2))/2 \quad (7)$$

4.2 Stereo Vision Calibration

In order to attain the precise coordinate of the markers on the patient body external, one key setback is precise calibration of constituents of the arrangement such as the video camera. In our arrangement, the camera is

believed as a pinhole model. The connection amid a point in the world coordinate construction and its corresponding pixel in the picture plane can be delineated as pursuing protrusion model:

$$sI = A[R, t]X \tag{8}$$

where $I = [r \ c \ 1]^T$ is the homogeneous coordinate of the pixel in the picture frame; $X = [x \ y \ z \ 1]^T$ is the homogeneous coordinate of the corresponding point in the globe frame; s is the scale factor; $[R, t]$ is the camera extrinsic parameter matrix representing the rotation and translation amid the camera construction and globe frame; A is the camera intrinsic parameter matrix and can be composed as:

$$A = \begin{bmatrix} \alpha & \gamma & r_0 \\ 0 & \beta & c_0 \\ 0 & 0 & 1 \end{bmatrix}$$

where r_0, c_0 is the coordinate of the principle point; α and β are the focal length alongside the r and c axes of the picture plane;

γ is the parameter representing the skew of the two picture axes. The camera is calibrated by employing Zhang's method . The flat checkerboard alongside 15x15mm gird size as shown Fig 5 is allocated at disparate locations and orientations and seized by the video camera

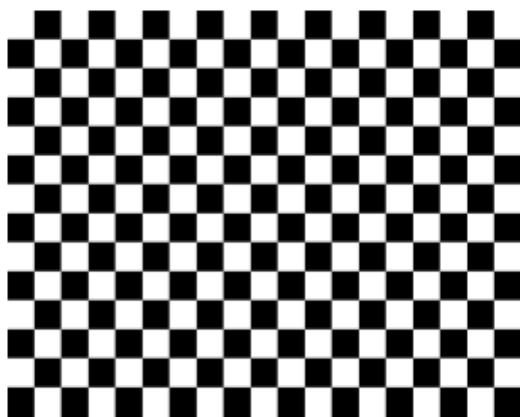


Fig. 5 The calibration checkerboard

The intrinsic parameter matrices A_1 and A_2 are obtained as:

$$A_1 = \begin{bmatrix} 2685.5 & 0 & 511.5 \\ 0 & 2662.8 & 383.5 \\ 0 & 0 & 1 \end{bmatrix}$$

$$A_2 = \begin{bmatrix} 2939.4 & 0 & 511.5 \\ 0 & 2914.4 & 383.5 \\ 0 & 0 & 1 \end{bmatrix}$$

After calibrating the video cameras, we demand to calibrate the finished examination system. For this patriotic, a uniform construction for the stereo vision arrangement is instituted alongside its x and y axes lied in the picture plane of one of the calibration pictures and its z axis perpendicular to the plane. The makeover amid this uniform construction and MTD transmitter construction next demand to be identified. In exercise, we use a stylus alongside a MTD receiver on it to recognize the coordinate of a little pre-defined markers in the MTD transmitter coordinate construction, as shown in Fig 6 . We can additionally become the coordinates of these markers in the stereo vision arrangement coordinate frame. PT is the marker coordinate in the MTD transmitter construction and PV is the marker coordinate in the stereo vision's uniform frame. Then, the corresponding makeover matrix M amid these two coordinates can be composed as

$$P_T = M \cdot P_V \tag{9}$$

Once the makeover matrix M has been calibrated, the coordinates of these markers on the patient's body external can be recognized in a real-time manner by employing stereo vision. So, the movement of wanted target can be noticed dynamically.

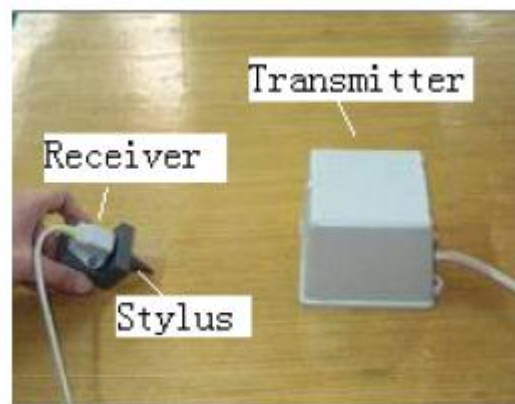


Fig. 6 The stylus calibration

5. EXPERIMENTS AND RESULTS

5.1 Stereo Vision Accuracy Test

To confirm the pursuing accuracy of the stereo vision arrangement, we set up an examination and examined a planar board alongside a cluster of markers. The measured data were fitted to a flawless plane by employing linear square method, as shown in Fig 7 (a). The distance amid the measured point and the fitted plane is the pursuing error corresponding to the marker. Fig 7 (b) is the computed stereo vision pursuing error. It can be discovered that the mean worth of the pursuing error is less than 0.16mm.

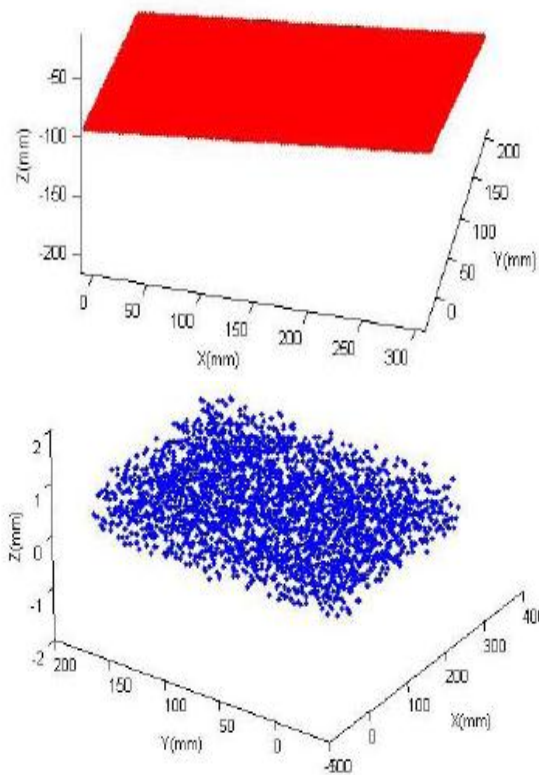


Fig. 7 3D ultrasound accuracy test

5.2 Navigation Arrangement Accuracy Test

In order to examination the accuracy of the counseled surgical exploration arrangement, we utilized a 3D ultrasound phantom as shown in Fig 8 (endowed by the Institute of Acoustics in the Chinese Academy of Science) to simulate the liver tissue and the clinical tumors. The external of the container was obscured by Plexiglas physical except the aural window (at the top of the container), that was composed of polyester film. The phantom container was loaded alongside tissue imitating physical (background), that was utilized to simulate the normal liver tissue and was displayed as

background in the US image. An array of target globes (1 cm in diameter) embedded in the tissue imitating physical was utilized to simulate the clinical tumors (target) in the liver. The background and the target physical have the alike sound speed parameter 1540 ± 10 m/s. But they have disparate attenuation coefficient: 0.7 dB/cm/MHz for the background physical and 0.35 dB/cm/MHz for the target sphere.

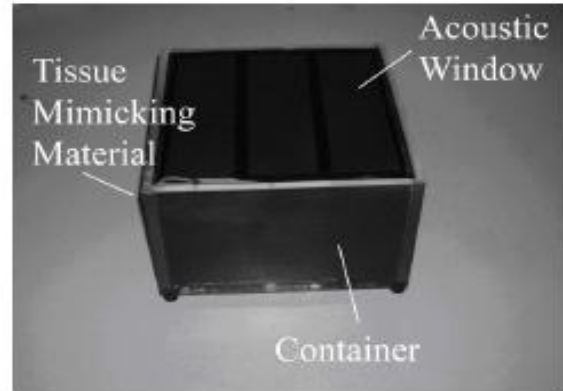


Fig. 8 3D Ultrasound Phantom

We utilized the procedure delineated in serving II for this test. In order to simulate the movement of the structure gave by respiratory gesture; we knowingly pressed the aural window, emerging in the movement of target spheres. The markers on the aural window (simulate the markers on the patient's body surface) should move simultaneously. The stereo vision arrangement should notice the magnitude and association of the gesture for every single marker and the arrangement should notify the surgeon that it was not the best period to present the surgery. We might adjust the target globes to a pre-defined locale (reference state) and uphold present state by thinking the US videos from the monitor, simulating the scenario that the patient holds his or her breath. Then, we inserted the average biopsy needle. The needle was calibrated beforehand the examination as shown in Fig 6 and its precise locale was displayed in the monitor. Below the education of the projected trajectory shown in Fig 9, the exploration arrangement computed the vector v joining present needed tip and the projected target point. The worth of the final distance $d = |v|$ was utilized to denote the error of the system. The error includes the error of 3D assembly, registration error, robot manipulation error and stereo vision pursuing error, etc.

After the procedure, the phantom was scanned once more to examination the result. Fig 10 gives one consequence of the needle insertion experiment. From

the figure, we can discern that the needle tip is extremely close to the center of target. The examination was recapped 20 periods, and the aftermath merely vary a slight amid every single test. The mean worth of the error is 2.13mm and the stand deviation is 1.45mm.

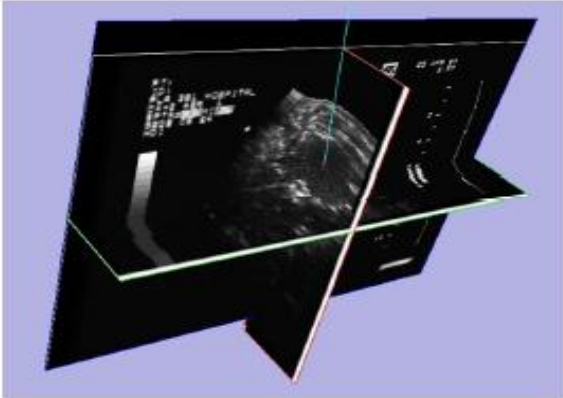


Fig. 9 The projected trajectory and target

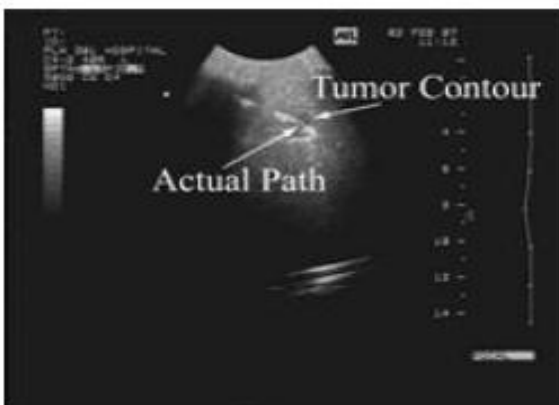


Fig. 10 The Consequence of Needle-insertion

6. CONCLUSION

In this paper, a robotic surgery exploration arrangement for the interventional radiology therapy of liver cancer has been developed. In order to enhance the accuracy of the needle insertion, we counseled a method to notice the movement of the structure gave by the patient's respiratory motion. First, a body fixation method is utilized to cut each comparative movement of the patient alongside respect to the robotic exploration system. Next, stereo vision method is utilized to notice the gesture of the body external comparative to the reference state. The counseled method can compensate the gesture or unexpected shivering of the target provoked by respiration or cardiac function. Therefore, probability of duty the target or each supplementary chance connected to the target movement can be minimized. With the combination of the multimedia exploration and robot gesture domination, it is probable to precisely adjust the needle trail according to a prior

projected trajectory. The needle feed is visualized in the patient's data set to confirm the needle placement. Such methods might make the needle inserting procedure extremely fast and accurate. The accuracy examination alongside a 3D ultrasound phantom illustrates that the repletion accuracy of the finished arrangement is in the scope of 2.13 ± 1.45 mm. The subsequent pace will involve a discover on animal prior to clinical evaluation.

REFERENCE

- [1] D.C Barratt, A.H Davies, A.D Hughes, S.A Thom and K.N. Humphries, Optimisation and evaluation of an electromagnetic tracking device for high accuracy three dimensional ultrasound imaging of the carotid arteries. *Ultrasound in Medicine and Biology*, 27 (7), 2001, 957-968.
- [2] R.A Beasley, *Model-Based Error Correction for Instrument Flexion in Robotic Surgery*, Doctoral Thesis, Harvard University, Cambridge, Massachusetts, 2006.
- [3] G.J.D. Bergman, Variation in the cervical range of motion over time measured by the flock of birds" *Electromagnetic Tracking System*, 30 (6), March 15, 2005, 650-654
- [4] E.M. Boctor, G. Fischer, M.A. Choti, G. Fichtinger and R.H. Taylor, A dual-armed robotic system for intraoperative ultrasound guided hepatic ablative therapy: A prospective study, *Proc. 2004 IEEE International Conference on Robotics & Automation*, New Orleans, LA, 2004.
- [5] E.M. Boctor, A. Jain, M.A. Choti, R.H. Taylor and G. Fichtner, A rapid calibration method for registration and 3d tracking of ultrasound images using spatial localizer. *Medical Imaging 2003: Ultrasonic Imaging and Signal Processing*, Proceedings of SPIE, 5035, 2003, 521-532.
- [6] E.M. Boctor, R.J. Webster, M.A. Choti, R.H. Taylor and G. Gichtinger, Robotically assisted ablative treatment guided by freehand 3D Ultrasound, *Proc. CARS*, Chicago, 2004.
- [7] D.F.B. France, J.D. Gallagher, J.M. Furman, M.S. Redfern and G.E. Carvell, Voluntary upper-extremity movements in patients with unilateral peripheral vestibular hypofunction. *Physical Therapy*, 82 (3), 2002, 217-227.
- [8] A.M.J. Bull and A.A. Amis, Accuracy of an Electromagnetic Tracking Device, *J. Biomech*, 30 (8), 1997, 857-858.
- [9] C. Calin, A. Silviu and G. Bogdan, A new three-dimensional mapping system for routine free hand ultrasound examinations, *Proc. 12th World*

Congress of the World Federation for Ultrasound in Medicine and Biology, 30 August - 3 September, 2009, Australia.

- [10] P. Cheng, H. Zhang, H. Kim, K. Gary, M.B. Blake, D. Gobbi, S. Aylward, J. Jomier, A. Enquobahrie, R. Avila, L. Ibanez and K. Cleary IGSTK: Framework and Example Application Using an Open Source Toolkit for Image-Guided Surgery Applications. *Proc. SPIE Medical Imaging*, Feb 11-16, 2006, San Diego, CA.